Purdue University

Purdue e-Pubs

CTRC Research Publications   Cooling Technologies Research Center

2020

The Effect of Channel Diameter on Flow Freezing in Microchannel

A. Jain

A. Miglani

J. A. Weibel

S V. Garimella

International Journal of Heat and Mass Transfer

The effect of channel diameter on flow freezing in microchannels

Aakriti Jain, Ankur Miglani, Justin A. Weibel, Suresh V. Garimella*

School of Mechanical Engineering, Purdue University, West Lafayette, IN 47907 USA

ARTICLE INFO

ABSTRACT

An understanding of the factors that affect the flow freezing process in microchannels is important in the development of microfluidic ice valves featuring well-controlled and fast response times. This study explores the effect of channel diameter on the flow freezing process and the time to achieve channel closure. The freezing process is experimentally investigated for a pressure-driven water flow (0.3 ml/min) through three glass microchannels with inner diameters of 500 μm, 300 μm, and 100 μm, respectively, using channel-wall temperature measurements synchronized with high-magnification, high-speed imaging. Freezing invariably initiates in supercooled water as a thin layer of dendritic ice that grows along the inner channel wall, followed by the formation and growth of a thick annular ice layer which ultimately causes complete channel closure. The growth time of the annular ice layer decreases monotonically with channel diameter, with the 100 μm channel having the shortest closing time. Specifically, the mean closing time for this smallest channel is measured to be 0.25 s, which is markedly shorter compared to other reports in the existing literature using larger channel sizes at similar flow rates. A model-based analysis of the freezing process is used to show that the total latent heat released by the freezing mass (which varies as the square of the channel diameter) is the key factor governing the closing time. Owing to this simple scaling, the study reveals that reducing the channel diameter offers an attractive approach to increasing the responsiveness of ice valves to achieve non-intrusive flow control at high sample flow rates.

1. Introduction

Microvalves are crucial components that enable complex functionality in microfluidic platforms through reliable flow management of the reagents, including routing, timing, and segregation. Ice valves hold particular promise as reliable microvalves because they freeze the working medium (aqueous solution) itself to shut off the flow. Thus, they need no external mechanical actuation, are leak-free at high pressure, have no dead volume [1], and do not introduce foreign materials into the system [2]. Fig. 1 shows a schematic diagram of ice valve formation mechanism in a channel exposed to a localized external wall temperature that is less than the equilibrium freezing temperature of the fluid. However, ice valves have a long response time due to the need to cool down the entire thermal mass of the system to a supercooled temperature before ice nucleation can occur. A number of existing studies have focused on modifying the microfluidic device design or the cooling method [1,3,4] to reduce the response time of ice valves. A few studies [5,6] have attempted to determine the factors that

govern the flow freezing process in small channels so as to guide strategies for reducing the closing time.

In our recent study [5], the modes of ice formation were characterized during flow freezing in a 500 μm inner-diameter channel. The effect of flow rate (0.5 to 1.5 ml/min) on the freezing process and the channel closing time was studied. It was observed that freezing always initiated in the dendritic mode, which caused partial flow obstruction, followed by the growth of annular ice that led to complete channel closure. Higher flow rates required lower external channel wall temperatures to cool down the liquid to its nucleation temperature within the given channel length ($l/D = 40$) due to the higher effective sensible heat capacity of the flow. This resulted in a larger temperature difference between the outer channel wall and the ice-water interface; this larger temperature difference available to drive the radial heat conduction resulted in a faster annular ice growth and a shorter closing time.

Because channel closure is caused by annular ice formation, previous studies have focused on developing models that predict the rate of annular ice growth to estimate the closing time. We recently developed [5] a volume-discretization-based model to determine the factors that influence annular ice growth. The model demonstrated that the annular ice growth rate is dictated by the rate at which the latent heat released during freezing can be con-

Nomenclature

D	channel inner diameter ($D = 2R$) [m]
k	thermal conductivity [W/mK]
l	channel length [m]
L	latent heat [J/kg]
m	mass of water in the channel [kg]
R	channel inner radius [m]
ΔR	change in radius over a time step [m]
t	time [s]
Δt	time step [s]
T	temperature [°C]
ΔT	temperature difference [°C]
z	axial or streamwise position along the channel centerline [m]
Δz	length of a unit control volume in the axial direction [m]

Greek symbols

ρ	density [kg/m^3]

Subscripts

ann	annular ice region
bs	borosilicate glass
cav	test cell cavity
calc	calculated
cl	closing
den	dendritic ice region
exp	experimental
ext	external
f	freezing
i	ice-water interface
int	internal
s	solid phase (ice)
TC	thermocouple reading
wall	channel wall

Superscript

i	index for a unit control volume
j	index for time step

ducted radially outward from the channel. Specifically, the annular closing time was predicted to vary inversely with the temperature difference driving the latent heat (which is indirectly controlled by the water flow rate), and directly with both the square of the channel diameter and the effective thermal resistance to radial heat flow. Myers and Low [7] developed a 2D model for predicting the annular ice growth in rectangular and circular microchannels using lubrication theory, under the assumption of a long and thin channel geometry. Their expression for the channel closing time also showed a functional dependence on the driving temperature difference and the channel hydraulic diameter. These models indicate that the channel closing time may be reduced either by increasing the temperature difference driving the radial conduction or by reducing the channel diameter. From a practical viewpoint, the latter is a simpler and more cost/energy-conscious approach compared to former which may require a more complex, higher power cooling system.

The current study aims to experimentally demonstrate that reducing the channel diameter is a promising approach to achieving fast channel closure using ice valves in microfluidic platforms. The effect of channel diameter on the channel closing time is characterized by investigating the flow freezing process using high-speed visualization synchronized with the external channel wall thermocouple readings for three channel inner diameters ($D = 100\ \mu$m,

300 μm, and 500 μm, respectively) at a constant-pressure-driven water flow rate of 0.3 ml/min. The channel closing times are determined visually from the high-magnification images. Based on a simplified annular ice growth model [5], the factors affecting the closing time are identified and the critical role of channel diameter is examined.

2. Experimental facility and procedures

The experimental facility and procedures used in this study are identical to those in our previous study [5], except for the additional channel diameters investigated. The key details are summarized in the Supplementary Materials. In this study, three different channel sizes are used with nominal inner diameters (D) of 500 μm, 300 μm, and 100 μm. These channels have a wall thickness ($R_{wall,ext} - R_{wall,int}$) of 100 μm, 50 μm, and 20 μm, respectively. Additionally, the constant-pressure driven flow rate of 0.3 ml/min is established for all channel sizes by pressurizing the reservoir according to the pressure drop in the channel.

3. Results and discussion

### 3.1. Effect of channel diameter on the ice formation modes and channel closing time

The flow freezing of water in microchannels of different diameters is presented here, including the measured temperature readings and visualizations of the freezing process after ice nucleates at the water-wall interface. The different ice formation modes are identified, and the channel closing time is measured for different channel diameters.

Fig. 2(a) and (b) show a time sequence of high-magnification images of the ice formation process for channel diameters of $D = 500\ \mu$m and 100 μm, respectively. These images show the process starting from the dendritic ice nucleation at the channel inside surface to complete closure of the channel by inward growth of annular ice. This process of dendritic ice growth followed by annular ice closure is observed in all three channel diameters, as shown in the high-speed videos in the Supplementary Materials; these materials also include a time sequence of images for the intermediate diameter, $D = 300\ \mu$m.

Dendritic ice nucleation occurs at the water-wall interface near the channel outlet. Following nucleation ($t = 0$ s), the dendritic ice grows rapidly along the channel wall in the axial upstream direction and covers the entire field-of-view within $t = 0.08$ s and 0.006 s for $D = 500\ \mu$m and 100 μm, respectively. Because dendritic ice is formed only in supercooled water [8–14], we infer that the water adjacent to the internal channel wall is supercooled.

As shown in Fig. 2(a) at $t = 0.04$ s, the dendritic ice growth along the inner front surface (i.e., in front of the focal plane) and the along the inner back surface (i.e., behind the focal plane) appears as two distinct layers. In addition, these distinct ice layers are not connected by any matrix of dendrites. Based on these visualizations, it can be inferred that the dendritic ice grows only as a thin layer adjacent to the wall and does not fill the entire channel cross-section. This behavior is consistent with many previous studies [13–16] on the growth of dendrites in supercooled water, which have shown that the dendritic ice tends to grow along a wall rather than into the bulk. This occurs because the channel wall has higher thermal diffusivity compared to the water and acts as a heat sink for the latent heat released during ice formation. In Fig. 2(b), a higher magnification (9.7$\times$ for $D = 100\ \mu$m compared to 2.3$\times$ for $D = 500\ \mu$m) is used due to the smaller channel size.

The dendritic ice nucleates when the wall temperature is below the equilibrium freezing point. Formation of dendritic ice is accompanied by latent heat release, which rapidly increases the wall
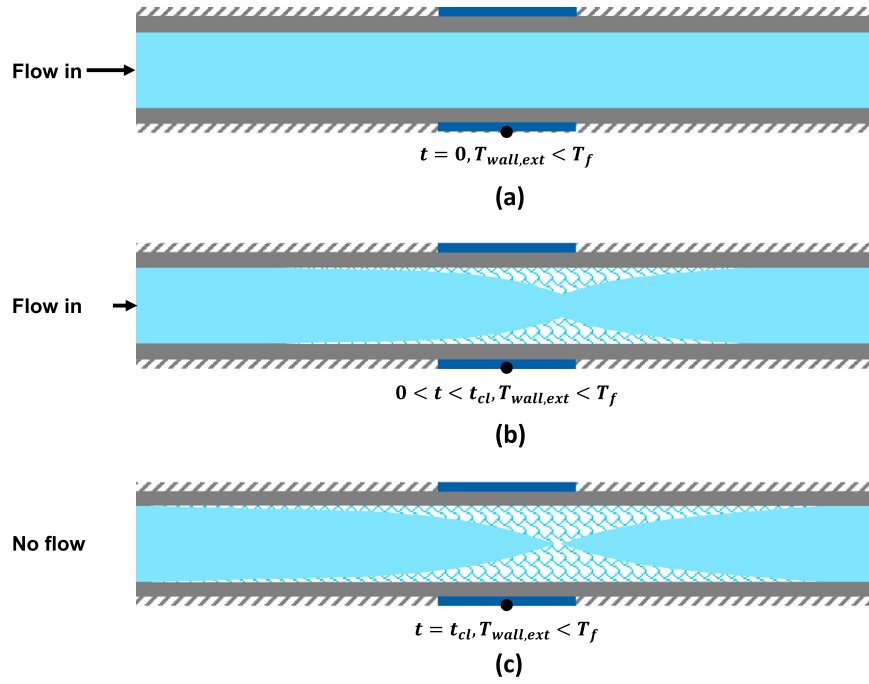
Fig. 1. Schematic diagram showing channel closure using an ice valve, where the channel is exposed to external wall temperature lower than the equilibrium freezing temperature.

temperature and brings the ice-water interface to the equilibrium freezing temperature. Fig. 3(a) shows a comparison of the time history of external channel wall thermocouple readings, $T_{wall,TC}$, during the freezing process for all 3 channel diameters. The data from each case are aligned in time such that $t = 0$ s corresponds to the instant of ice nucleation. The short delay observed between the ice nucleation and the rise in temperature readings is due to the finite amount of time taken by the dendritic ice to traverse the channel length along the wall and reach the inlet where the temperature is measured. As the dendritic ice grows on the wall, latent heat is released continuously, and the temperature begins to climb until it stabilizes at an almost constant value (e.g., approximately $-1.79°C$ at $t = 0.65$ s for $D = 500$ μm) when the entire channel length is covered with dendritic ice. The annular ice layer then becomes visible and grows radially inward (see Fig. 2(a)). As the annular ice grows and becomes substantially thicker such that the channel is nearing closure (e.g., at ~3 s in Fig. 2(a) for $D = 500$ μm), the ice begins to lose sensible heat and the temperature reading starts to drop. The annular ice then continues to grow radially inwards until it fills the entire cross-section at the closure plane. Closure occurs at $t = 3.48$ s for $D = 500$ μm and much sooner at $t = 0.25$ s for $D = 100$ μm. The annular closure front then moves both upstream and downstream of the closure plane until entire channel is blocked. In Fig. 3(a), it should be noted that the temperatures measured by the thermocouples, $T_{wall,TC}$, are expected to be lower than the actual external wall temperature during the annular ice growth periods, especially for $D = 300$ μm and 100 μm, as is further discussed in Section 3.2.

Fig. 3(b) shows a comparison of the channel closing times for all 3 channel diameters. The closing time is measured directly from the high-speed videos, starting from the frame which shows the dendritic ice nucleation to the frame where the annular ice fronts meet and block the channel. For each case, the observed variation in closing time is reported over the 8 repeated experimental trials. The median value of closing time (t_{cl}) decreases monotonically with channel diameter, viz., from 3.48 s for $D = 500$ μm to 1.38 s for $D = 300$ μm to 0.25 s for $D = 100$ μm. The minimum

closing time is shorter than previously reported values in the literature of 18 s [17] and 4.1 s [2] using a single-stage thermoelectric (TE) module and 2.27 s [3] using a two-stage TE cooling module. The only comparable closing time of 0.37 s was obtained using a large-footprint, multi-stage TE module at a much lower water flow rate of 10 μl/min [1]. This shortest reported closing time of 0.25 s obtained in the smallest 100 μm inner diameter channel is a critical demonstration showing that reducing the channel diameter is a viable and effective method of reducing the channel closing time. For ice valve applications, this approach may be a simpler alternative to introducing new cooling mechanisms or nucleating agents [4,18] to reduce the closing time.

3.2. Model-based analysis of the role of channel diameter on the annular ice growth time

We previously developed a simplified flow freezing model [5] that described the transient annular ice growth process and identified the key factors governing annular ice growth, and therefore, the channel closing time. Utilizing the model, this section analyzes the role of channel diameter in affecting the channel closing time.

In the model described in detail in Ref. [5], a channel with an external and an internal radius of $R_{wall,ext}$ and $R_{wall,int}$, respectively, is axially discretized into small control volumes of length Δz, each encompassing the entire cross-section. Within this control volume, the region occupied by the water is assumed to behave as a lumped mass. The channel external wall temperature, $T_{wall,ext}$, is at a uniform value lower than the equilibrium freezing temperature, T_f, along the entire length. Time is discretized in steps of Δt. An annular ice layer with the interface at $R_i^{i,j}$ (annular layer thickness = $R_{wall,int} - R_i^{i,j}$) and interface temperature T_i exists in a single control volume i at time step j. A small mass of water adjacent to the interface freezes and forms a solid ice layer of thickness $\Delta R_i^{i,j}$ over a time step Δt.

For each control volume, the model accounts for mass conservation (between the inlet mass flow, the outlet mass flow, and the
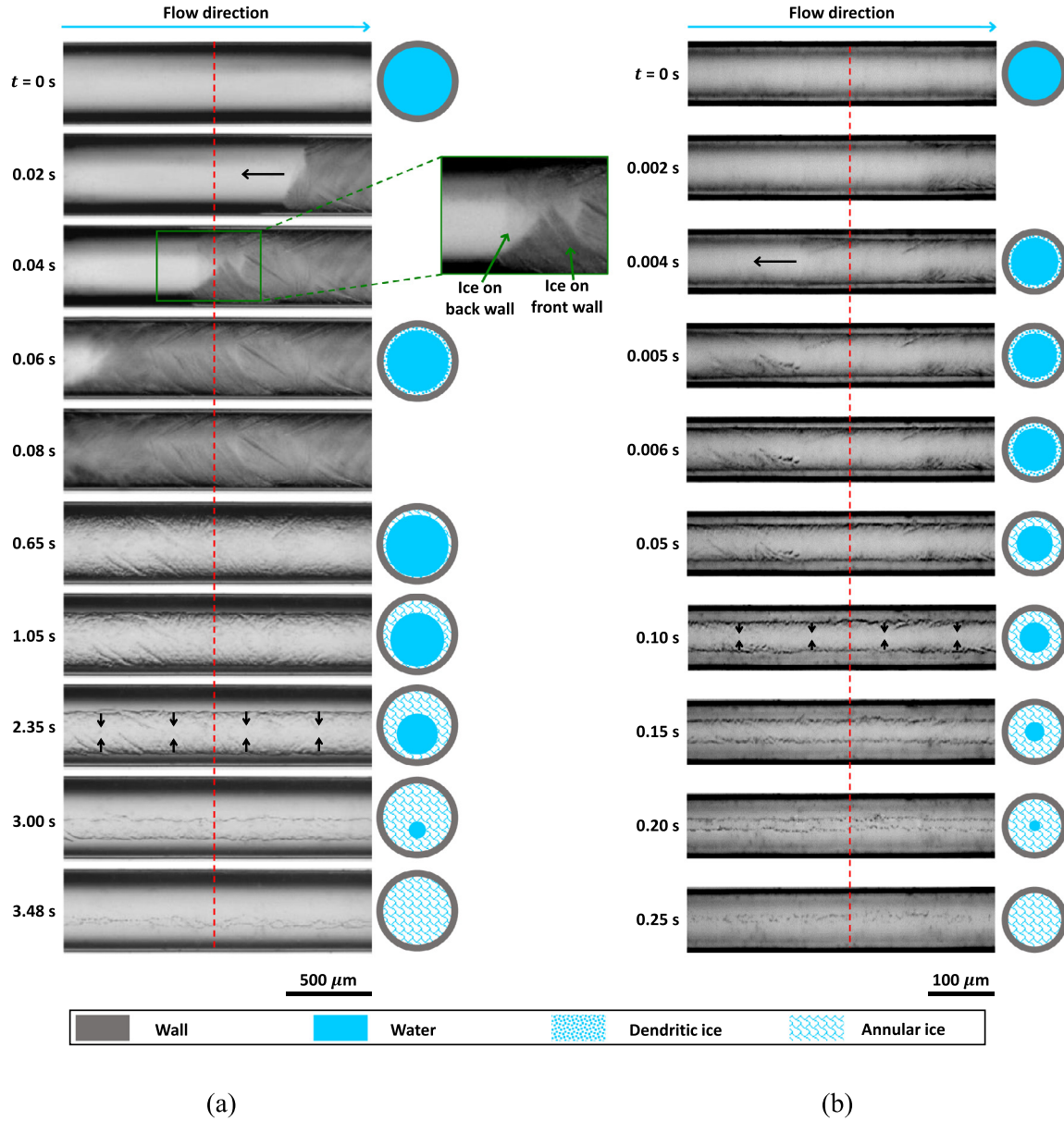
Fig. 2. Time sequence of images showing ice formation modes during flow freezing in a microchannel for (a) $D = 500$ μm and (b) $D = 100$ μm. The schematic diagrams to the right of the channels show the channel cross-section at the closure plane (dashed red line). The channel wall, water, dendritic ice, and annular ice regions are shaded as indicated in the legend. Flow direction is from left to right. The black arrows indicate the direction of ice growth. The scale bar for each channel diameter is indicated at the bottom.

mass of water frozen) as well as the energy conservation (between the energy advected along with the water flow, the latent heat released by the freezing mass, and the energy conducted radially outward from the channel) to calculate the location of the annular ice front at each time step. An order-of-magnitude comparison between the different energy terms shows that the annular ice growth is governed by the radial conduction of the released latent heat while the advection term has negligible effect on the freezing process (see the supplementary material of Ref. [5]).

The details of the modeling assumptions, simplification of the governing equations, and the solution algorithm can be found in Ref. [5]. The resultant expression for annular ice growth in the control volume i at time step j is given by:

$$\rho_s 2\pi R_i^{i,j} \frac{\Delta R_i^{i,j}}{\Delta t} \Delta z L_f \approx -2\pi \Delta z \frac{\left(T_i - T_{wall,ext}\right)}{\frac{\ln\left(R_{wall,int}/R_i^{i,j}\right)}{k_s} + \frac{\ln\left(R_{wall,ext}/R_{wall,int}\right)}{k_{bs}}} \quad (1)$$

Eq. (1) indicates that the growth rate of annular ice is determined by how fast the latent heat released during the freezing process can be conducted radially outward from the channel. An expression for the annular ice growth time (t_{ann}) can be obtained by integrating Eq. (1) with respect to R_i from $R_i = R_{wall,int}$ (at $t = 0$) to $R_i = 0$ (at $t = t_{ann}$).

$$t_{ann} \approx \frac{1}{\left(T_i - T_{wall,ext}\right)} \rho_s 2\pi \, \Delta z \frac{R_{wall,int}^2}{2} L_f$$

$$\times \left(\frac{1}{2k_s} + \frac{\ln\left(R_{wall,ext}/R_{wall,int}\right)}{k_{bs}}\right) \frac{1}{2\pi \, \Delta z} \quad (2)$$

Eq. (2) shows that the annular ice growth time is a function of three factors: (1) the driving temperature difference ($T_i - T_{wall,ext}$); (2) the total latent heat released by the freezing mass of water ($\rho_s \pi \Delta z R_{wall,int}^2 L_f$); and (3) the effective

Table 1
Comparison of the factors affecting the channel closing time for all channel diameters.

Parameters	Magnitudes		
Internal channel radius, $R_{wall,int}$ (μm)	250	150	50
External channel radius, $\boldsymbol{R_{wall,ext}}$ (μm)	350	200	70
Released latent heat, $\rho_s \pi \Delta z R_{wall,int}^2 L_f$ (J)	6.01×10^{-4}	2.16×10^{-4}	0.24×10^{-4}
Thermal resistance, $\left(\frac{1}{2k_s} + \frac{\ln(R_{wall,ext}/R_{wall,int})}{k_{bs}}\right)\frac{1}{2\pi\Delta z}$ (K/W)	0.85×10^4	0.78×10^4	0.85×10^4
Experimental annular ice growth time, $\boldsymbol{t_{ann}}$ ($= \boldsymbol{t_{cl}} - \boldsymbol{t_{den}}$) (s)	3.03	1.08	0.17
Calculated driving temperature difference, $\boldsymbol{T_i} - \boldsymbol{T_{wall,ext, calc}}$ ($^\circ$C)	1.69	1.57	1.23
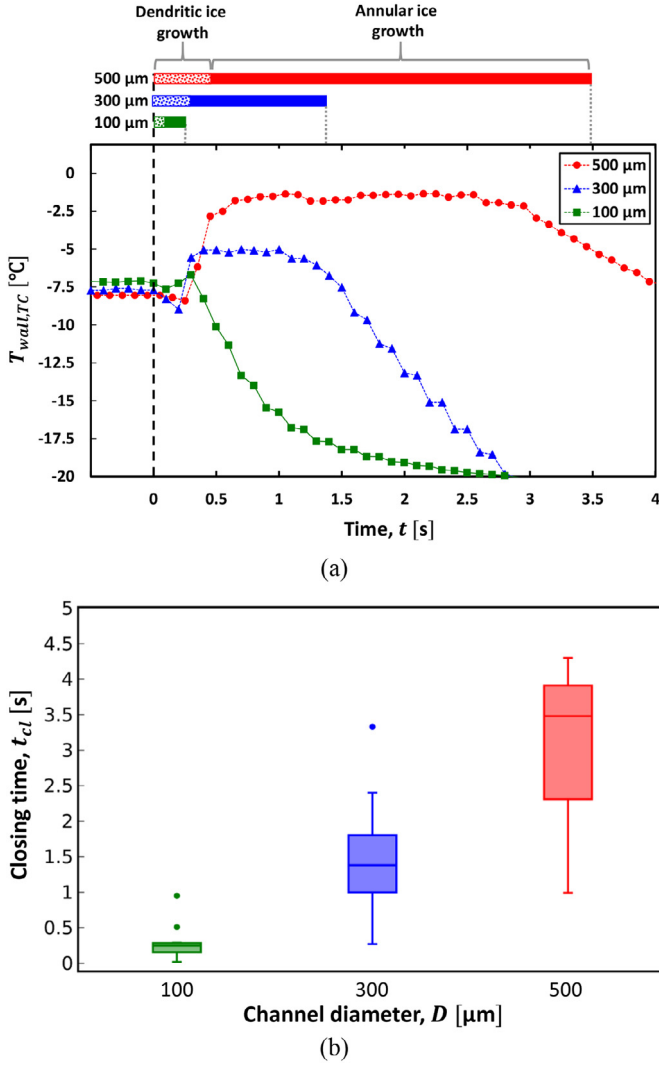
Fig. 3. (a) Temporal variation of the external channel wall thermocouple readings during the freezing process and beyond for all three channel diameters. The dashed black line represents the appearance of dendritic ice in the visualizations, marking the time of nucleation ($t = 0$ s). The bars on top show a comparison of the growth time of dendritic and annular ice obtained from flow visualization for each case. The dotted lines at the end of each bar represent channel closure. (b) Variation of the channel closing time as a function of the channel inner diameter, with variations shown over 8 repeated trials. The boxes span the first to third quartiles, while the horizontal lines inside the box represent the medians. The dots represent statistical outliers.

thermal resistance to radial flow of the released latent heat ($\{(1/2k_s) + [\ln(R_{wall,ext}/R_{wall,int})/k_{bs}]\} /2\pi\Delta z$). Table 1 shows the values of these factors for all 3 channel diameters.

Taking $T_i = 0$ °C and substituting $T_{wall,ext}$ with the experimentally measured value $T_{wall,\ TC}$ in Eq. (2) would lead to shorter clos-

ing times compared to the experimental observations from the high-speed images. As mentioned in Section 3.1, the temperature recorded by the thermocouple is expected to be lower than the actual external wall temperature driving the annular closure (i.e., an overestimate of the driving temperature difference). The thermocouple, which is not located directly at the point of initial ice nucleation or closure, reads lower than the actual external wall temperature primarily due to the delayed thermal response. This is particularly true for channels with $D = 300$ μm and 100 μm, which have faster annular ice growth rates and smaller thermal masses, such that a thick annulus of ice forms and the channel begins to lose sensible heat before any change in the thermocouple temperature is recorded. This is exemplified by a very small rise (0.2°C) in the wall thermocouple reading followed by a quick drop for $D = 100$ μm, as shown in Fig. 3(a).

To obtain an estimate of the actual external wall temperature driving the annular ice growth from the model, Eq. (2) can be rearranged as

$$T_{wall,ext,calc} \approx T_i - \frac{1}{t_{ann}} \rho_s 2\pi \Delta z \frac{R_{wall,int}^2}{2} L_f$$

$$\times \left(\frac{1}{2k_s} + \frac{\ln\left(R_{wall,ext}/R_{wall,int}\right)}{k_{bs}}\right) \frac{1}{2\pi \Delta z} \qquad (3)$$

On substituting the values of constants and annular ice growth time (t_{ann}) from the experiments (see Table 1) in Eq. (3), the external channel wall temperature is calculated as $T_{wall,ext,calc} = -1.69$ °C for $D = 500$ μm, which is close to the experimentally measured external wall thermocouple reading ($T_{wall,TC} = -1.79$ °C). For $D = 300$ μm and 100 μm, $T_{wall,ext,calc}$ is calculated to be -1.57°C and -1.23°C, respectively. Based on these values, the driving temperature difference for $D = 500$ μm is 1.45 times that for $D = 100$ μm, and the thermal resistance to the radial heat flow is the same for both these channel diameters. However, the total latent heat released for $D = 500$ μm is 25 times more than that for $D = 100$ μm, due to the difference in the quantity of water that needs to be frozen to attain channel closure. This implies that for a given flow rate, the total latent heat released, and hence the channel diameter, is indeed the dominating factor that governs the annular closing time.

4. Conclusions

The freezing of water flowing through glass microchannels ($D = 500$ μm, 300 μm, and 100 μm) is experimentally characterized to understand the effect of the channel diameter on the channel closing times, for potential microfluidic ice valve applications. The following key conclusions are drawn from the present study:

- Flow freezing occurs via the formation and growth of both dendritic and annular modes of ice formation that are observed with all three channel diameters (500 μm, 300 μm, and 100 μm). Freezing initiates as dendritic ice that grows along

the channel wall, followed by the formation and growth of annular ice that causes complete flow blockage and ultimate channel closure.

- The closing time is observed to decrease monotonically with a decrease in the channel diameter. An extremely short closing time of only 0.25 s is observed for the 100 μm channel at a flow rate of 0.3 ml/min.
- For a given water flow rate, the annular ice growth rate, and hence the channel closing time, is (1) directly proportional to the amount of total latent heat released during the freezing process (which varies as the square of the channel diameter) and (2) the thermal resistance to the radial conduction of this latent heat, while it is (3) inversely proportional to the temperature difference between the external wall temperature and the ice-water interface which drives the radial conduction of the released latent heat.
- For the investigated channel diameters, a comparison of the magnitudes of all the parameters shows that the total latent heat released by the freezing mass in the channel is the dominant term, which directly controls the annular closing time. The mass of freezing water varies as the square of the channel diameter and, hence, the closing time reduces significantly as the channel diameter is decreased.

The design of ice valves for microfluidic platforms must consider the channel size, the driving temperature difference, and the thermal resistance to heat flow. In our previous study [5], it was shown that for a given channel size a faster closure can be achieved by increasing the flow rate, which indirectly increases the driving temperature difference. The current study demonstrates that fast closure can also be achieved by reducing the channel diameter, which may offer a simpler approach, especially for microfluidic applications where using high flow rates or operating at very low temperatures to initiate freezing may not be feasible.

Declaration of Competing Interest

We wish to confirm that there are no known conflicts of interest associated with this publication and there has been no significant financial support for this work that could have influenced its outcome.

Supplementary materials

Supplementary material associated with this article can be found, in the online version, at doi:10.1016/j.ijheatmasstransfer.2020.119718.

References

[1] C. Si, S. Hu, X. Cao, W. Wu, High response speed microfluidic ice valves with enhanced thermal conductivity and a movable refrigeration source, Sci. Rep. 7 (2017) 40570.

[2] Z. Chen, J. Wang, S. Qian, H.H. Bau, Thermally-actuated, phase change flow control for microfluidic systems, Lab. Chip 5 (11) (2005) 1277–1285.

[3] L. Gui, J. Liu, Ice valve for a mini/micro flow channel, J. Micromechanics Microengineering 14 (2) (2004) 242.

[4] J.C. Gaiteri, W.H. Henley, N.A. Siegfried, T.H. Linz, J.M. Ramsey, Use of ice-nucleating proteins to improve the performance of freeze–thaw valves in microfluidic devices, Anal. Chem. 89 (11) (2017) 5998–6005.

[5] A. Jain, A. Miglani, Y. Huang, J.A. Weibel, S.V. Garimella, Ice formation modes during flow freezing in a small cylindrical channel, Int. J. Heat Mass Transf. 128 (2019) 836–848.

[6] A. Jain, Y. Huang, J.A. Weibel, S.V. Garimella, Visualization of ice formation modes and flow blockage during freezing of water flowing in a microchannel ASME 2016 Heat Transfer Summer Conference, 2016 paper HT2016–7243.

[7] T.G. Myers, J. Low, An approximate mathematical model for solidification of a flowing liquid in a microchannel, Microfluid. Nanofluidics 11 (4) (2011) 417–428.

[8] R.R. Gilpin, The effects of dendritic ice formation in water pipes, Int. J. Heat Mass Transf. 20 (6) (1977) 693–699.

[9] R.R. Gilpin, The effect of cooling rate on the formation of dendritic ice in a pipe with no main flow, J. Heat Transf. 99 (3) (1977) 419–424.

[10] R.R. Gilpin, Modes of ice formation and flow blockage that occur while filling a cold pipe, Cold Reg. Sci. Technol. 5 (2) (1981) 163–171.

[11] H. Inaba, K. Takeya, S. Nozu, Fundamental study on continuous ice making using flowing supercooled water, JSME Int. J. Ser. B 37 (2) (1994) 385–393.

[12] S.L. Braga, J.J. Milón, Visualization of dendritic ice growth in supercooled water inside cylindrical capsules, Int. J. Heat Mass Transf. 55 (13–14) (2012) 3694–3703.

[13] C.S. Lindenmeyer, G.T. Orrok, K.A. Jackson, B. Chalmers, Rate of growth of ice crystals in supercooled water, J. Chem. Phys. 27 (3) (1957) 822.

[14] H.R. Pruppacher, Growth modes of ice crystals in supercooled water and aqueous solutions, J. Glaciol. 6 (47) (1967) 651–662.

[15] W. Kong, H. Liu, A theory on the icing evolution of supercooled water near solid substrate, Int. J. Heat Mass Transf. 91 (2015) 1217–1236.

[16] J.G. Vlahakis, A.J. Bardhun, Growth rate of an ice crystal in flowing water and salt solutions, Am. Inst. Chem. Eng. J. 20 (3) (1974) 581–591.

[17] L. Gui, J. Liu, Ice valve for a mini/micro flow channel, J. Micromechanics Microengineering 14 (2) (2004) 242.

[18] J.M. Ramsey, W.H. Henley, J.C. Gaiteri, Fluidic devices with freeze-thaw valves with ice-nucleating agents and related methods of operation and analysis, US Patent No 20180200720 (2018).